

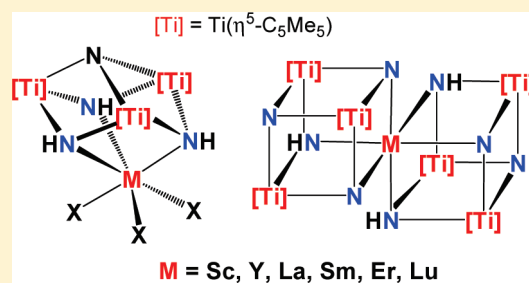
Molecular Nitrides with Titanium and Rare-Earth Metals

Jorge Caballo, María García-Castro, Avelino Martín, Miguel Mena, Adrián Pérez-Redondo, and Carlos Yélamos*

Departamento de Química Inorgánica, Universidad de Alcalá, 28871 Alcalá de Henares-Madrid, Spain

Supporting Information

ABSTRACT: A series of titanium-group 3/lanthanide metal complexes have been prepared by reaction of $[\{\text{Ti}(\eta^5\text{-C}_5\text{Me}_5)(\mu\text{-NH})\}_3(\mu_3\text{-N})]$ (**1**) with halide, triflate, or amido derivatives of the rare-earth metals. Treatment of **1** with metal halide complexes $[\text{MCl}_3(\text{thf})_n]$ or metal trifluoromethanesulfonate derivatives $[\text{M}(\text{O}_3\text{SCF}_3)_3]$ at room temperature affords the cube-type adducts $[\text{X}_3\text{M}\{(\mu_3\text{-NH})_3\text{Ti}_3(\eta^5\text{-C}_5\text{Me}_5)_3(\mu_3\text{-N})\}]$ ($\text{X} = \text{Cl}$, $\text{M} = \text{Sc}$ (**2**), Y (**3**), La (**4**), Sm (**5**), Er (**6**), Lu (**7**); $\text{X} = \text{OTf}$, $\text{M} = \text{Y}$ (**8**), Sm (**9**), Er (**10**)). Treatment of yttrium (**3**) and lanthanum (**4**) halide complexes with 3 equiv of lithium 2,6-dimethylphenoxido $[\text{LiOAr}]$ produces the aryloxo complexes $[(\text{ArO})_3\text{M}\{(\mu_3\text{-NH})_3\text{Ti}_3(\eta^5\text{-C}_5\text{Me}_5)_3(\mu_3\text{-N})\}]$ ($\text{M} = \text{Y}$ (**11**), La (**12**)). Complex **1** reacts with 0.5 equiv of rare-earth bis(trimethylsilyl)amido derivatives $[\text{M}\{(\text{SiMe}_3)_2\text{N}\}_3]$ in toluene at 85–180 °C to afford the corner-shared double-cube nitrido compounds $[\text{M}(\mu_3\text{-N})_3(\mu_3\text{-NH})_3\{\text{Ti}_3(\eta^5\text{-C}_5\text{Me}_5)_3(\mu_3\text{-N})\}_2]$ ($\text{M} = \text{Sc}$ (**13**), Y (**14**), La (**15**), Sm (**16**), Eu (**17**), Er (**18**), Lu (**19**)) via $\text{NH}(\text{SiMe}_3)_2$ elimination. A single-cube intermediate $[\{\text{M}(\text{SiMe}_3)_2\text{N}\}\text{Sc}\{(\mu_3\text{-N})_2(\mu_3\text{-NH})\text{Ti}_3(\eta^5\text{-C}_5\text{Me}_5)_3(\mu_3\text{-N})\}]$ (**20**) was obtained by the treatment of **1** with 1 equiv of the scandium bis(trimethylsilyl)amido derivative $[\text{Sc}\{(\text{SiMe}_3)_2\text{N}\}_3]$. The X-ray crystal structures of **2**, **7**, **11**, **14**, **15**, and **19** have been determined. The thermal decomposition in the solid state of double-cube nitrido complexes **14**, **15**, and **18** has been investigated by thermogravimetric analysis (TGA) and differential thermal analysis (DTA) measurements, as well as by pyrolysis experiments at 1100 °C under different atmospheres (Ar, H_2/N_2 , NH_3) for the yttrium complex **14**.



INTRODUCTION

Polynuclear transition-metal nitrido complexes constitute a class of molecular cage compounds with fascinating structures and interesting bonding properties.¹ While nitrido complexes of the mid transition-metals (groups 6, 7, and 8) in a high oxidation state are usually mononuclear and feature terminal nitrido ligands,² in early transition-metal (groups 4 and 5) systems there is a stronger tendency to form dimeric or oligomeric species with nitrido ligands bridging two or more metal centers. Structurally characterized examples include di-,^{3,4} tri-,^{5,6} tetra-,⁷ penta-,⁸ and hexanuclear⁹ complexes with nitrido moieties shared between the metal centers. In those examples, the presence of bulky ancillary ligands (e.g., cyclopentadienyl, alkoxido) at the metal centers is crucial to obtain discrete and soluble molecular compounds. Species with μ_n -nitrido groups are proposed as intermediates in dinitrogen fixation and activation,^{10–12} and new structural and electronic data on molecular systems may provide insights into those processes.

Interest in the development of polynuclear nitrido complexes is also due to their potential role as building blocks and precursors of metal nitride (MN) materials.¹³ Although the literature precedents are still scarce, Wolczanski and co-workers have demonstrated that the geometry of the nitrido tantalum precursor $[(\text{tBuCH}_2)_2\text{TaN}]_5 \cdot \text{NH}_3 \cdot 2\text{C}_7\text{H}_8$ allows access to cubic TaN at 820 °C, instead of the hexagonal phase, which is more thermodynamically stable at that temperature.^{8a,14} In this

context, molecular heterometallic nitrido compounds with preformed $\text{M}-\text{N}-\text{M}'$ linkages are attractive candidates to serve as precursors of ternary metal nitrides,¹⁵ or homogeneous ceramic composites consisting of two or more binary nitrides. Thermal decomposition of heterobimetallic precursors with well-defined structures can offer a unique and facile approach for the preparation of materials with optimum distribution of both metals. The advantage of this method over the classical multicomponent approach has recently been demonstrated for the preparation of heterobimetallic oxide materials from organometallic cage precursors.¹⁶ A review of the literature shows several examples of the use of molecular or polymeric precursors in the synthesis of ternary metal nitrides or homogeneous nitride composites,^{13,17} but the search reveals also the lack of systematic strategies for the rational construction of aggregates with desired metal compositions.

As part of a project devoted to the development of polynuclear nitrido complexes, we have been investigating the rational synthesis of a family of heterometallic nitrido complexes by treatment of the trinuclear titanium imido-nitrido complex $[\{\text{Ti}(\eta^5\text{-C}_5\text{Me}_5)(\mu\text{-NH})\}_3(\mu_3\text{-N})]$ ^{4,6} (**1**) with a variety of metal derivatives. Compound **1** shows an incomplete-cube $[\text{Ti}(\mu\text{-NH})_3(\mu_3\text{-N})]$ core and is prone to incorporate metal fragments

Received: April 25, 2011

Published: June 16, 2011

into the structure to give cube-type heterometallic complexes. The sterically demanding pentamethylcyclopentadienyl groups on the titanium atoms of **1** are crucial to confer solubility and stability to those polynuclear nitrido complexes, enabling to uncover a diverse spectrum of chemical structure and reactivity in this area. Our previous work has shown that **1** is capable of acting as a neutral chelate ligand through the basal NH groups toward transition¹⁸ and main-group¹⁹ metal derivatives. We have also recently reported the preliminary results on the coordination of **1** to yttrium and erbium halides.²⁰ In those complexes, **1** acts as a facially coordinating ligand to the rare-earth centers and resembles other six-electron donors as the anionic tris(pyrazolyl)borates,²¹ the neutral analogous tris(pyrazolyl)methanes and tris(pyrazolyl)silanes,^{22,23} and cyclic triamines such as 1,4,7-triazacyclononanes^{23,24} and 1,3,5-triazacyclohexanes.^{23b,25} Herein we report a systematic study on the coordination of the metal-ligand **1** to group 3 and lanthanide metals, as well as preliminary experiments on the solid-state thermal decomposition of several molecular nitrides with titanium and rare-earth metals.

EXPERIMENTAL SECTION

General Considerations. All manipulations were carried out under argon atmosphere using Schlenk line or glovebox techniques. Toluene and hexane were distilled from Na/K alloy just before use. Tetrahydrofuran (THF, thf) was distilled from purple solutions of sodium benzophenone just prior to use. NMR solvents were dried with Na/K alloy (C₆D₆) or calcium hydride (CDCl₃) and vacuum-distilled. Oven-dried glassware was repeatedly evacuated with a pumping system (ca. 1 × 10⁻³ Torr) and subsequently filled with inert gas. Thermolyses in solution at high temperatures were carried out by heating flame-sealed NMR or Carius tubes in a Roth autoclave model III. Anhydrous group 3 and lanthanide metal halides [MCl₃] were purchased from Aldrich or Strem and used as received. The thf adducts [MCl₃(thf)_n]²⁶ (M = Sc, Lu, n = 3; M = Y, Sm, Er, n = 3.5; M = La,²⁷ n = 1.5) were prepared by heating under reflux a suspension of [MCl₃] in THF. Metal tris(trifluoromethanesulfonate) reagents [M(O₃SCF₃)₃] (M = Y, La, Sm, Er) were purchased from Aldrich, and heated at 180 °C under dynamic vacuum prior to use. Lithium 2,6-dimethylphenoxido [Li(OAr)] was prepared by reaction of 2,6-dimethylphenol with [LinBu] (Aldrich, 1.6 M in hexane). [(Ti(η⁵-C₅Me₅)(μ-NH)₃(μ₃-N)] (**1**),^{4,6} [Y(CH₂SiMe₃)₃(thf)₃]²⁸ and [M{N(SiMe₃)₂}]₃ (M = Sc,²⁹ Y, La, Sm, Eu, Lu)³⁰ were prepared according to published procedures. The syntheses and characterization of complexes **3** and **6** have been reported previously.²⁰

Samples for infrared spectroscopy were prepared as KBr pellets. ¹H, ¹³C{¹H}, and ¹⁹F NMR spectra were recorded on a Varian Unity-300 and/or Mercury-300 spectrometers. Chemical shifts (δ, ppm) in the ¹H and ¹³C{¹H} NMR spectra are given relative to residual protons or to carbon of the solvent. Chemical shifts (δ, ppm) in the ¹⁹F NMR spectra are given relative to CFC₃ as external reference. Microanalyses (C, H, N, S, O) were performed in a Leco CHNSO-932 microanalyzer. Simultaneous DTA/TG analysis were conducted on a SDT Q600 TA Instruments coupled with quadrupole mass spectrometer system (THERMOSTAR GSD300 T3) at the Instituto de Ciencias de Materiales de Madrid ICMM-CSIC. Samples were heated between 25 and 1000 °C using argon as the flow gas (200 sccm) with a heating rate of 10 °C/min (sample weights ≈ 10 mg). SEM/EDX results were obtained on a Hitachi TM-1000 instrument with SwiftED-TM. Powder X-ray diffraction (PXRD) analyses were performed on a Bruker Model D8 Advance diffractometer using Cu Kα radiation (λ = 1.5418 Å).

Synthesis of [Cl₃Sc{(μ₃-NH)₃Ti₃(η⁵-C₅Me₅)₃(μ₃-N)}] (2**).** A 100 mL Schlenk flask was charged with **1** (0.30 g, 0.49 mmol), [ScCl₃(thf)₃] (0.18 g, 0.49 mmol), toluene (20 mL) and THF

(5 mL). The reaction mixture was stirred at room temperature for 24 h to give an orange solid and a brown solution. The solid was isolated by filtration onto a glass frit and vacuum-dried to afford **2** as an orange powder (0.26 g, 70%). IR (KBr, cm⁻¹): ν̄ 3331 (s), 2912 (s), 1487 (w), 1426 (m), 1380 (s), 1067 (w), 1024 (w), 730 (vs), 708 (vs), 664 (s), 643 (vs), 619 (s), 535 (w), 476 (w), 436 (w). ¹H NMR (CDCl₃, 20 °C): δ 12.31 (s br., 3H; NH), 2.17 (s, 45H; C₅Me₅). ¹³C{¹H} NMR (CDCl₃, 20 °C): δ 125.0 (C₅Me₅), 12.6 (C₅Me₅). Anal. Calcd for C₃₀H₄₈Cl₃N₄ScTi₃ (M_w = 759.65): C 47.43, H 6.37, N 7.38. Found: C 47.21, H 6.00, N 6.97.

Synthesis of [Cl₃La{(μ₃-NH)₃Ti₃(η⁵-C₅Me₅)₃(μ₃-N)}] (4**).** In a fashion similar to the preparation of **2**, the treatment of **1** (0.50 g, 0.82 mmol) with [LaCl₃(thf)_{1.5}] (0.28 g, 0.78 mmol) in toluene (20 mL) and THF (5 mL) afforded **4** as a yellow powder (0.52 g, 78%). IR (KBr, cm⁻¹): ν̄ 3310 (s), 2909 (s), 2859 (m), 1489 (m), 1427 (s), 1378 (s), 1066 (w), 1025 (m), 758 (s), 695 (vs), 663 (vs), 532 (w), 475 (m), 431 (w). ¹H NMR (CDCl₃, 20 °C): δ 13.37 (s br., 3H; NH), 2.17 (s, 45H; C₅Me₅). ¹³C{¹H} NMR (CDCl₃, 20 °C): δ 123.7 (C₅Me₅), 12.7 (C₅Me₅). Anal. Calcd for C₃₀H₄₈Cl₃LaN₄Ti₃ (M_w = 853.61): C 42.21, H 5.67, N 6.56. Found: C 41.82, H 5.30, N 6.36.

Synthesis of [Cl₃Sm{(μ₃-NH)₃Ti₃(η⁵-C₅Me₅)₃(μ₃-N)}] (5**).** In a fashion similar to the preparation of **2**, the treatment of **1** (0.30 g, 0.49 mmol) with [SmCl₃(thf)_{3.5}] (0.25 g, 0.49 mmol) in toluene (20 mL) and THF (5 mL) at room temperature for 24 h gave **5** as a yellow powder (0.35 g, 83%). IR (KBr, cm⁻¹): ν̄ 3312 (s), 2909 (s), 1488 (m), 1427 (s), 1377 (s), 1066 (w), 1023 (m), 861 (w), 701 (vs), 656 (vs), 532 (w), 475 (m), 431 (w). ¹H NMR (CDCl₃, 20 °C): δ 13.55 (s br., 3H; NH), 1.99 (s, 45H; C₅Me₅). ¹³C{¹H} NMR (CDCl₃, 20 °C): δ 123.4 (C₅Me₅), 12.3 (C₅Me₅). Anal. Calcd for C₃₀H₄₈Cl₃N₄SmTi₃ (M_w = 865.06): C 41.65, H 5.59, N 6.48. Found: C 41.43, H 5.69, N 6.25.

Synthesis of [Cl₃Lu{(μ₃-NH)₃Ti₃(η⁵-C₅Me₅)₃(μ₃-N)}] (7**).** In a fashion similar to the preparation of **2**, the treatment of **1** (0.20 g, 0.33 mmol) with [LuCl₃(thf)₃] (0.17 g, 0.33 mmol) in toluene (20 mL) and THF (5 mL) at room temperature for 24 h afforded **7** as a yellow powder (0.16 g, 55%). IR (KBr, cm⁻¹): ν̄ 3329 (s), 2912 (s), 2859 (m), 1485 (m), 1425 (s), 1380 (s), 1066 (w), 1024 (w), 775 (s), 736 (vs), 701 (vs), 643 (vs), 620 (vs), 535 (m), 477 (m), 436 (w), 407 (w). ¹H NMR (CDCl₃, 20 °C): δ 12.50 (s br., 3H; NH), 2.17 (s, 45H; C₅Me₅). ¹³C{¹H} NMR (CDCl₃, 20 °C): δ 124.4 (C₅Me₅), 12.3 (C₅Me₅). Anal. Calcd for C₃₀H₄₈Cl₃LuN₄Ti₃ (M_w = 889.66): C 40.50, H 5.44, N 6.30. Found: C 40.52, H 5.25, N 6.31.

Synthesis of [(CF₃SO₂O)₃Y{(μ₃-NH)₃Ti₃(η⁵-C₅Me₅)₃(μ₃-N)}] (8**).** A 100 mL Schlenk flask was charged with **1** (0.30 g, 0.49 mmol), [Y(O₃SCF₃)₃] (0.24 g, 0.44 mmol), and toluene (30 mL). The reaction mixture was stirred at room temperature for 2 days. The brown suspension was filtered through a coarse glass frit, and the resultant orange solid in the frit was vacuum-dried and characterized as **8** (0.36 g, 72%). IR (KBr, cm⁻¹): ν̄ 3329 (w), 3294 (w), 2920 (w), 1429 (w), 1383 (m), 1338 (vs), 1240 (vs), 1196 (vs), 1036 (vs), 1014 (s), 763 (m), 635 (vs), 512 (m), 477 (w). ¹H NMR (CDCl₃, 20 °C): δ 13.16 (s br., 3H; NH), 2.18 (s, 45H; C₅Me₅). ¹³C{¹H} NMR (CDCl₃, 20 °C): δ 124.0 (C₅Me₅), 12.1 (C₅Me₅). ¹⁹F NMR (CDCl₃, 20 °C): δ -77.9. Anal. Calcd for C₃₃H₄₈F₉N₄O₉S₃·Ti₃Y (M_w = 1144.45): C 34.63, H 4.23, N 4.90, S 8.41. Found: C 34.85, H 4.72, N 4.85, S 7.95.

Synthesis of [(CF₃SO₂O)₃Sm{(μ₃-NH)₃Ti₃(η⁵-C₅Me₅)₃(μ₃-N)}] (9**).** In a fashion similar to the preparation of **8**, the treatment of **1** (0.30 g, 0.49 mmol) with [Sm(O₃SCF₃)₃] (0.28 g, 0.47 mmol) in toluene (30 mL) at 70 °C for 2 days afforded **9** as an orange solid (0.44 g, 77%). IR (KBr, cm⁻¹): ν̄ 3325 (w), 3289 (w), 2920 (w), 1489 (w), 1429 (w), 1383 (w), 1337 (s), 1237 (vs), 1195 (vs), 1030 (vs), 1010 (vs), 758 (s), 635 (vs), 594 (w), 536 (w), 512 (s), 476 (m), 440 (m). ¹H NMR (CDCl₃, 20 °C): δ 13.87 (s br., 3H; NH), 2.01 (s, 45H; C₅Me₅). ¹³C{¹H} NMR (CDCl₃, 20 °C): δ 125.3 (C₅Me₅), 12.0

(C₅Me₅). ¹⁹F NMR (CDCl₃, 20 °C): δ -77.5. Anal. Calcd for C₃₃H₄₈F₉N₄O₉S₃SmTi₃ (M_w = 1205.90): C 32.87, H 4.01, N 4.65, S 7.98. Found: C 31.02, H 3.93, N 4.40, S 7.52.

Synthesis of [(CF₃SO₂O)₃Er{(μ₃-NH)₃Ti₃(η⁵-C₅Me₅)₃(μ₃-N)}] (**10**). In a fashion similar to the preparation of **8**, the treatment of **1** (0.30 g, 0.49 mmol) with [Er(O₃SCF₃)₃] (0.29 g, 0.47 mmol) in toluene (30 mL) at room temperature for 2 days afforded **10** as an orange solid (0.46 g, 81%). IR (KBr, cm⁻¹): ν̄ 3329 (w), 3294 (w), 2920 (w), 1489 (w), 1429 (w), 1383 (m), 1339 (vs), 1241 (vs), 1196 (vs), 1036 (vs), 1013 (s), 763 (m), 635 (vs), 596 (w), 537 (w), 512 (m), 477 (w), 441 (w), 410 (w). Anal. Calcd for C₃₃H₄₈ErF₉N₄O₉S₃·Ti₃ (M_w = 1222.80): C 32.41, H 3.96, N 4.58, S 7.87. Found: C 32.21, H 4.14, N 4.34, S 8.29.

Synthesis of [(ArO)₃Y{(μ₃-NH)₃Ti₃(η⁵-C₅Me₅)₃(μ₃-N)}] (**11**). A 100 mL Schlenk flask was charged with **3** (0.30 g, 0.37 mmol), lithium 2,6-dimethylphenoxido (0.14 g, 1.12 mmol), and toluene (50 mL). The reaction mixture was stirred at ambient temperature for 24 h to give an orange solution and a white fine powder. After filtration, the volatile components of the solution were removed under reduced pressure to afford **11** as a yellow solid (0.37 g, 95%). IR (KBr, cm⁻¹): ν̄ 3347 (s), 2944 (s), 2911 (s), 2856 (s), 1592 (s), 1468 (vs), 1427 (vs), 1377 (s), 1299 (vs), 1279 (vs), 1240 (s), 1092 (s), 1025 (w), 976 (w), 917 (w), 859 (s), 799 (m), 746 (vs), 703 (s), 676 (vs), 656 (vs), 562 (w), 530 (s), 477 (m), 433 (w). ¹H NMR (CDCl₃, 20 °C): δ 13.33 (s br, 3H; NH), 6.76 (d, ³J_{HH} = 7.5 Hz, 6H; OC₆H₂HMe₂), 6.36 (t, ³J_{HH} = 7.5 Hz, 3H; OC₆H₂HMe₂), 2.08 (s, 45H; C₅Me₅), 2.00 (s, 18H; OC₆H₂HMe₂). ¹³C{¹H} NMR (CDCl₃, 20 °C): δ 161.7 (d, ²J_{CY} = 4.9 Hz; *ipso*-OC₆H₂HMe₂), 127.4 (*m*-OC₆H₂HMe₂), 125.6 (*o*-OC₆H₂HMe₂), 122.5 (C₅Me₅), 114.4 (*p*-OC₆H₂HMe₂), 18.7 (OC₆H₂HMe₂), 11.9 (C₅Me₅). Anal. Calcd for C₅₄H₇₅N₄O₃Ti₃Y (M_w = 1060.71): C 61.15, H 7.13, N 5.28. Found: C 61.13, H 6.81, N 5.07.

Synthesis of [(ArO)₃La{(μ₃-NH)₃Ti₃(η⁵-C₅Me₅)₃(μ₃-N)}] (**12**). In a fashion similar to the preparation of **11**, the treatment of **4** (0.30 g, 0.35 mmol) with lithium 2,6-dimethylphenoxido (0.14 g, 1.05 mmol) in toluene (50 mL) at room temperature for 24 h afforded **12** as a yellow solid (0.32 g, 82%). IR (KBr, cm⁻¹): ν̄ 3336 (m), 2910 (s), 1591 (s), 1465 (vs), 1425 (vs), 1377 (m), 1293 (vs), 1274 (vs), 1237 (vs), 1090 (m), 1025 (w), 974 (w), 915 (w), 851 (m), 746 (vs), 697 (m), 667 (vs), 654 (vs), 526 (m), 476 (m), 432 (w). ¹H NMR (CDCl₃, 20 °C): δ 13.59 (s br, 3H; NH), 6.80 (d, ³J_{HH} = 7.5 Hz, 6H; OC₆H₂HMe₂), 6.37 (t, ³J_{HH} = 7.5 Hz, 3H; OC₆H₂HMe₂), 2.07 (s, 45H; C₅Me₅), 2.04 (s, 18H; OC₆H₂HMe₂). ¹³C{¹H} NMR (CDCl₃, 20 °C): δ 163.1 (*ipso*-OC₆H₂HMe₂), 127.3 (*m*-C₆H₂HMe₂), 125.1 (*o*-OC₆H₂HMe₂), 122.0 (C₅Me₅), 114.3 (*p*-OC₆H₂HMe₂), 18.5 (OC₆H₂HMe₂), 11.8 (C₅Me₅). Anal. Calcd for C₅₄H₇₅LaN₄O₃Ti₃ (M_w = 1110.71): C 58.39, H 6.81, N 5.04. Found: C 58.16, H 6.84, N 4.75.

Synthesis of [Sc{(μ₃-N)₃(μ₃-NH)₃{Ti₃(η⁵-C₅Me₅)₃(μ₃-N)}]₂] (**13**). A 100 mL Carius tube was charged with **1** (0.30 g, 0.49 mmol), [Sc{N(SiMe₃)₂}₃] (0.13 g, 0.25 mmol), and toluene (15 mL). The tube was flame-sealed and heated at 180 °C for 4 days. The reaction mixture was allowed to cool to ambient temperature overnight to afford red crystals. The tube was opened in the glovebox, and the crystals were collected by filtration and characterized as **13**·2C₇H₈ (0.26 g, 72%) according to analytical data. IR (KBr, cm⁻¹): ν̄ 3345 (m), 2905 (s), 2854 (s), 2717 (w), 1604 (w), 1494 (w), 1434 (m), 1373 (s), 1079 (w), 1023 (w), 804 (w), 720 (vs), 640 (vs), 620 (vs), 590 (s), 531 (w), 487 (w), 464 (w), 418 (s). Anal. Calcd for C₇₄H₁₀₉N₈ScTi₆ (M_w = 1442.89): C 61.60, H 7.61, N 7.77. Found: C 61.02, H 7.60, N 7.71.

Synthesis of [Y{(μ₃-N)₃(μ₃-NH)₃{Ti₃(η⁵-C₅Me₅)₃(μ₃-N)}]₂] (**14**). A 100 mL ampule (Teflon stopcock) was charged with **1** (1.00 g, 1.64 mmol), [Y{N(SiMe₃)₂}₃] (0.47 g, 0.82 mmol), and toluene (20 mL). The reaction mixture was heated at 110 °C without any stirring for 7 days, and the solution was allowed to cool to ambient

temperature overnight to afford dark green crystals of **14**·2C₇H₈ (1.04 g, 85%). IR (KBr, cm⁻¹): ν̄ 3336 (w), 2905 (s), 2854 (s), 2718 (w), 1604 (w), 1494 (w), 1432 (s), 1373 (s), 1156 (w), 1066 (w), 1023 (w), 803 (w), 720 (vs), 694 (s), 671 (vs), 657 (vs), 636 (vs), 621 (vs), 528 (w), 464 (w), 418 (m), 400 (m). Anal. Calcd for C₇₄H₁₀₉N₈Ti₆Y (M_w = 1486.84): C 59.78, H 7.39, N 7.54. Found: C 59.39, H 7.04, N 7.41.

Synthesis of [La{(μ₃-N)₃(μ₃-NH)₃{Ti₃(η⁵-C₅Me₅)₃(μ₃-N)}]₂] (**15**). In a fashion similar to the preparation of **14**, the treatment of **1** (1.00 g, 1.64 mmol) with [La{N(SiMe₃)₂}₃] (0.51 g, 0.82 mmol) in toluene (20 mL) at 85 °C for 7 days afforded orange crystals of **15** (0.95 g, 86%). IR (KBr, cm⁻¹): ν̄ 3326 (w), 2905 (s), 2855 (s), 2719 (w), 1602 (w), 1492 (m), 1434 (s), 1373 (s), 1075 (m), 1024 (m), 801 (m), 717 (vs), 691 (vs), 619 (vs), 530 (m), 468 (m), 447 (w). Anal. Calcd for C₆₀H₉₃LaN₈Ti₆ (M_w = 1352.56): C 53.28, H 6.93, N 8.28. Found: C 53.90, H 6.99, N 7.79.

Synthesis of [Sm{(μ₃-N)₃(μ₃-NH)₃{Ti₃(η⁵-C₅Me₅)₃(μ₃-N)}]₂] (**16**). In a fashion similar to the preparation of **14**, the treatment of **1** (0.30 g, 0.49 mmol) with [Sm{N(SiMe₃)₂}₃] (0.16 g, 0.25 mmol) in toluene (20 mL) at 110 °C for 2 days afforded orange crystals of **16**·C₇H₈ (0.19 g, 53%). IR (KBr, cm⁻¹): ν̄ 3331 (w), 2906 (s), 2849 (s), 1602 (w), 1494 (w), 1432 (m), 1374 (s), 1023 (w), 714 (vs), 692 (vs), 670 (vs), 620 (vs), 528 (m), 471 (m), 412 (m). Anal. Calcd for C₆₇H₁₀₁N₈SmTi₆ (M_w = 1456.15): C 55.26, H 6.99, N 7.70. Found: C 55.05, H 6.77, N 7.64.

Synthesis of [Eu{(μ₃-N)₃(μ₃-NH)₃{Ti₃(η⁵-C₅Me₅)₃(μ₃-N)}]₂] (**17**). In a fashion similar to the preparation of **14**, the treatment of **1** (0.15 g, 0.25 mmol) with [Eu{N(SiMe₃)₂}₃] (0.078 g, 0.12 mmol) in toluene (20 mL) at 100 °C for 4 days afforded brown crystals of **17** (0.082 g, 51%). IR (KBr, cm⁻¹): ν̄ 3331 (w), 2906 (s), 2854 (s), 1494 (w), 1434 (m), 1374 (s), 1066 (w), 1023 (w), 802 (w), 721 (vs), 693 (vs), 654 (vs), 621 (vs), 584 (m), 527 (w), 471 (w), 442 (w), 417 (w). Anal. Calcd for C₆₀H₉₃EuN₈Ti₆ (M_w = 1365.62): C 52.77, H 6.86, N 8.21. Found: C 52.75, H 6.78, N 8.44.

Synthesis of [Er{(μ₃-N)₃(μ₃-NH)₃{Ti₃(η⁵-C₅Me₅)₃(μ₃-N)}]₂] (**18**). In a fashion similar to the preparation of **13**, the treatment of **1** (0.30 g, 0.49 mmol) with [Er{N(SiMe₃)₂}₃] (0.16 g, 0.25 mmol) in toluene (20 mL) at 180 °C for 24 h afforded **18**·2C₇H₈ as brown crystals (0.31 g, 79%). IR (KBr, cm⁻¹): ν̄ 3334 (w), 2905 (s), 2855 (s), 1604 (w), 1491 (w), 1436 (m), 1373 (m), 1073 (w), 1023 (w), 941 (w), 810 (w), 722 (vs), 617 (s), 527 (m), 470 (w), 416 (s). Anal. Calcd for C₇₄H₁₀₉ErN₈Ti₆ (M_w = 1565.19): C 56.79, H 7.02, N 7.16. Found: C 56.41, H 6.49, N 6.88.

Synthesis of [Lu{(μ₃-N)₃(μ₃-NH)₃{Ti₃(η⁵-C₅Me₅)₃(μ₃-N)}]₂] (**19**). In a fashion similar to the preparation of **14**, the treatment of **1** (0.30 g, 0.49 mmol) with [Lu{N(SiMe₃)₂}₃] (0.16 g, 0.24 mmol) in toluene (20 mL) at 110 °C for 24 h gave **19**·C₇H₈ as dark green crystals (0.27 g, 75%). IR (KBr, cm⁻¹): ν̄ 3339 (w), 2905 (s), 2854 (s), 2718 (w), 1604 (w), 1493 (m), 1435 (s), 1373 (m), 1067 (m), 1023 (m), 875 (w), 804 (m), 721 (s), 694 (s), 673 (w), 636 (s), 617 (s), 588 (m), 526 (m), 476 (w), 419 (s). Anal. Calcd for C₆₇H₁₀₁LuN₈Ti₆ (M_w = 1480.76): C 54.35, H 6.87, N 7.57. Found: C 54.91, H 7.15, N 7.10.

Synthesis of [Y{(Me₃Si)₂N}Sc{(μ₃-N)₂(μ₃-NH)Ti₃(η⁵-C₅Me₅)₃(μ₃-N)}] (**20**). A 100 mL ampule (Teflon stopcock) was charged with **1** (0.30 g, 0.49 mmol), [Sc{N(SiMe₃)₂}₃] (0.26 g, 0.49 mmol), and toluene (30 mL). The reaction mixture was stirred at 100 °C for 3 days to give a dark red solution. The volatile components of the solution were removed under reduced pressure, and the resultant deep red solid was vacuum-dried and characterized as **20** (0.35 g, 88%). IR (KBr, cm⁻¹): ν̄ 3340 (w), 2909 (vs), 2857 (s), 2722 (w), 1493 (w), 1437 (m), 1376 (s), 1244 (s), 1179 (w), 1067 (w), 1024 (m), 986 (vs), 875 (vs), 846 (vs), 832 (vs), 782 (m), 754 (w), 704 (vs), 664 (vs), 632 (vs), 619 (vs), 555 (s), 472 (w), 458 (w), 436 (m), 417 (m). ¹H NMR (C₆D₆, 20 °C): δ 11.44 (s br, 1H; NH), 2.16 (s, 15H; C₅Me₅), 2.02 (s, 30H; C₅Me₅), 0.28 (s, 18H; SiMe₃). ¹³C{¹H} NMR (C₆D₆, 20 °C): δ 118.7 (C₅Me₅), 118.2

Table 1. Experimental Data for the X-ray Diffraction Studies on **2**, **7**, **11**, **14**, **15**, and **19**

	2	7	11 ·0.5C ₆ H ₁₄	14 ·2C ₇ H ₈	15	19 ·2C ₇ H ₈
formula	C ₃₀ H ₄₈ Cl ₃ N ₄ ScTi ₃	C ₃₀ H ₄₈ Cl ₃ LuN ₄ Ti ₃	C ₅₇ H ₈₂ N ₄ O ₃ Ti ₃ Y	C ₇₄ H ₁₀₉ N ₈ Ti ₆ Y	C ₆₀ H ₉₃ LaN ₈ Ti ₆	C ₇₄ H ₁₀₉ LuN ₈ Ti ₆
M _r	759.73	889.74	1103.88	1487.00	1352.73	1573.06
T [K]	200(2)	200(2)	200(2)	200(2)	200(2)	200(2)
λ [Å]	0.71073	0.71073	0.71073	0.71073	0.71073	0.71073
crystal system	monoclinic	monoclinic	monoclinic	orthorhombic	monoclinic	orthorhombic
space group	P2 ₁ /c	P2 ₁ /c	P2 ₁ /c	Pnmm	C2/c	Pnmm
a [Å]	11.175(3)	11.118(3)	12.443(2)	14.717(1)	27.961(6)	14.654(1)
b [Å]; β [deg]	17.723(3); 94.17(4)	17.895(3); 94.20(2)	21.245(2); 110.97(2)	15.433(5)	11.588(1); 106.13(2)	15.439(4)
c [Å]	37.034(11)	37.373(5)	23.112(6)	16.701(5)	20.911(5)	16.711(4)
V [Å ³]	7315(3)	7416(3)	5705(2)	3793(2)	6509(2)	3781(1)
Z	8	8	4	2	4	2
ρ _{calcd} [g cm ⁻³]	1.380	1.594	1.285	1.302	1.380	1.382
μ _{MoKα} [mm ⁻¹]	1.053	3.503	1.456	1.399	1.381	1.938
F(000)	3152	3552	2324	1560	2792	1624
crystal size [mm ³]	0.21 × 0.14 × 0.11	0.18 × 0.13 × 0.11	0.32 × 0.26 × 0.16	0.29 × 0.22 × 0.14	0.31 × 0.19 × 0.13	0.33 × 0.18 × 0.16
θ range (deg)	3.01 to 27.51	3.17 to 25.02	3.00 to 27.50	5.07 to 25.24	5.04 to 27.51	3.22 to 27.53
index ranges	−14 to 14, −23 to 23, 0 to 48	−13 to 13, −21 to 21, 0 to 44	−16 to 15, −27 to 27, −30 to 15	−17 to 17, −18 to 18, 0 to 20	−36 to 34, −15 to 15, 0 to 27	−19 to 19, −20 to 20, 0 to 21
reflections collected	123787	129009	121012	59932	67603	44357
unique data	16798 [R(int) = 0.105]	13041 [R(int) = 0.094]	13088 [R(int) = 0.033]	3530 [R(int) = 0.075]	7396 [R(int) = 0.059]	4487 [R(int) = 0.100]
obsd data [I > 2σ(I)]	8559	7829	9286	2847	4911	2988
goodness-of-fit on F ²	1.004	1.032	1.096	1.115	1.046	1.046
final R ^a indices [I > 2σ(I)]	R1 = 0.074, wR2 = 0.165	R1 = 0.069, wR2 = 0.163	R1 = 0.041, wR2 = 0.106	R1 = 0.096, wR2 = 0.237	R1 = 0.056, wR2 = 0.125	R1 = 0.074, wR2 = 0.193
R ^a indices (all data)	R1 = 0.162, wR2 = 0.206	R1 = 0.125, wR2 = 0.194	R1 = 0.070, wR2 = 0.117	R1 = 0.118, wR2 = 0.251	R1 = 0.100, wR2 = 0.142	R1 = 0.113, wR2 = 0.213
largest diff. peak/hole [e Å ⁻³]	1.076 and −1.042	1.707 and −2.007	0.463 and −0.460	1.141 and −0.577	1.027 and −0.571	1.428 and −1.444

^aR1 = Σ||F_o| − |F_c||/Σ|F_o|, wR2 = {Σw(F_o² − F_c²)/Σw(F_o²)^{1/2}}.

(C₅Me₅), 12.2 (C₅Me₅), 12.1 (C₅Me₅), 5.2 (SiMe₃). Anal. Calcd for C₃₆H₆₄N₅ScSi₂Ti₃ (M_w = 811.67): C 53.27, H 7.95, N 8.63. Found: C 53.05, H 8.18, N 8.24.

X-ray Structure Determination of **2, **7**, **11**, **14**, **15**, and **19**.** Crystals of complexes **2** and **7** were obtained by slow diffusion of a THF solution of [MCl₃(thf)₃] in toluene solutions of **1**. Crystals of compound **11**·0.5C₆H₁₄ were grown at room temperature by diffusion of hexane into a toluene solution of **11**. Crystals of complexes **14**·2C₇H₈, **15**, and **19**·2C₇H₈ were obtained by slow cooling of heated toluene solutions of a mixture of the reagents **1** and [M{N(SiMe₃)₂}]₃ as described above. The crystals were removed from the Schlenk flasks and covered with a layer of a viscous perfluoropolyether (FomblinY). A suitable crystal was selected with the aid of a microscope, attached to a glass fiber, and immediately placed in the low temperature nitrogen stream of the diffractometer. The intensity data sets were collected at 200 K on a Bruker-Nonius KappaCCD diffractometer equipped with an Oxford Cryostream 700 unit. Crystallographic data for all the complexes are presented in Table 1.

The structures were solved, using the WINGX package,³¹ by direct methods (SHELXS-97) and refined by least-squares against F² (SHELXL-97).³² Crystals of **2** and **7** contained two independent molecules in the asymmetric unit, and there were no significant differences between them. All non-hydrogen atoms were anisotropically

refined. All hydrogen atoms of **2** and **7** were positioned geometrically and refined using a riding model in the last cycles of refinement. DELU restraints were applied for the carbon atoms C(31)–C(35) and C(41)–C(45) of two pentamethylcyclopentadienyl ligands in complex **7**.

Compound **11** crystallized with a half molecule of hexane. Several attempts to obtain chemically sensible models for the solvent failed, so the PLATON³³ squeeze procedure was used to remove their contribution to the structure factors. All non-hydrogen atoms were anisotropically refined. All the hydrogen atoms were positioned geometrically and refined by using a riding model, except those of the imido groups (H(12), H(13), H(23)), which were located in the difference Fourier map and refined isotropically.

Complexes **14** and **19** crystallized with two molecules of toluene in the Pnmm space group. Attempts to model the solvent in a sensible way also failed and similarly to **11**, the PLATON³³ squeeze procedure was applied. Simultaneously, some of the carbon atoms of the pentamethylcyclopentadienyl rings linked to Ti(2) [C(21), C(24), C(26) and C(29) for **14**, and C(21), C(24), C(25) and C(29) for **19**] presented disorder, and were refined in two sites with occupancy 50%. However, the disorder did not affect the location of the core of the molecule. All non-hydrogen atoms of **14** were anisotropically refined, except the C(21), C(26), C(27), C(28) and C(29) carbon atoms of the disordered C₅Me₅ group. Similarly to **14**, all non-hydrogen atoms of **19** were anisotropically

refined, except the carbon atoms (C(21), C(22), C(23), C(24), C(25), C(26), C(28) and C(29)) of the disordered C₅Me₅ ring linked to Ti(2). On the other hand, compound **15** crystallized as a solvent-free molecule in the C2/c space group. The molecule lies on a crystallographic inversion center situated on the lanthanum atom. All non-hydrogen atoms were anisotropically refined. Finally, all hydrogen atoms of **14**, **15** and **19** were included, positioned geometrically, and refined by using a riding model. The imido hydrogen atoms were statistically distributed over the six nitrogen atoms linked to the central yttrium, lanthanum, or lutetium atom (final 50% of occupancy).

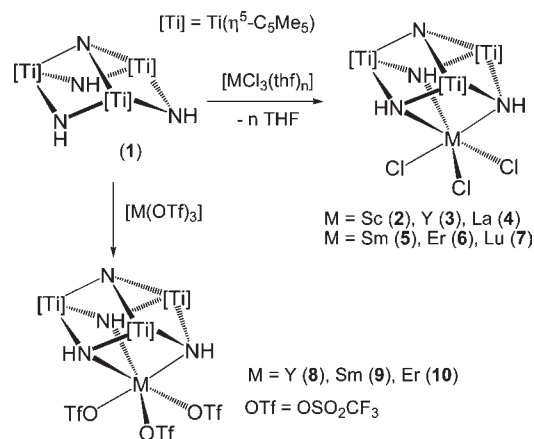
Pyrolysis of 14. In an argon-filled glovebox, an alumina boat was charged with a pulverized sample of compound **14**·C₇H₈ (0.20 g). The boat was placed in the middle point of a quartz tube (2.5 cm diameter × 40 cm length) equipped with two 24/40 male glass joints. The tube was fitted with 24/40 vacuum adapters (Teflon stopcock), and then inserted into a horizontal tube furnace (Lindberg Blue M). The oven was heated from 20 to 1100 °C with a heating rate of 5 °C/min under Ar (U–N45, O₂ ≤ 2 ppm, and H₂O ≤ 3 ppm), H₂/N₂ (6–15% of H₂, O₂ < 5 ppm, and H₂O < 5 ppm) or NH₃ (N50, O₂ < 1 ppm, and H₂O < 1 ppm) flows of 100 or 1350 sccm (cm³/min). The temperature was maintained at 1100 °C for 1 h, and the tube was allowed to cool to ambient temperature under a constant flow of the corresponding gas. The tube was taken into the glovebox, and the residue was manipulated under argon atmosphere. In the pyrolysis experiment under H₂/N₂ flow, the volatile decomposition products were subsequently trapped at –196 °C (N₂ liquid bath) in a cooling trap, and after closing the flow of gas, benzene-*d*₆ was injected into the cooling flask. The resultant C₆D₆ solution was analyzed by ¹H NMR spectroscopy and GC-MS measurements.

RESULTS AND DISCUSSION

Reactions with Rare-Earth Metal Halide and Triflate Derivatives. The synthetic chemistry is outlined in Scheme 1. Treatment of [$\{\text{Ti}(\eta^5\text{-C}_5\text{Me}_5)(\mu\text{-NH})\}_3(\mu_3\text{-N})$] (**1**) with 1 equiv of group 3 or lanthanide trichloride adducts [MCl₃(thf)_{*n*}] (M = Sc, Lu, *n* = 3; M = Y, Sm, Er, *n* = 3.5; M = La, *n* = 1.5) in a 4:1 toluene-THF mixture at room temperature afforded the precipitation of the cube-type complexes [Cl₃M{($\mu_3\text{-NH}$)₃Ti₃($\eta^5\text{-C}_5\text{Me}_5$)₃($\mu_3\text{-N}$)}] (M = Sc (**2**), Y (**3**), La (**4**), Sm (**5**), Er (**6**), Lu (**7**)) as orange or yellow solids in good yields (55–83%). Compounds **2–7** are not soluble in benzene, toluene or THF but exhibit a good solubility in halogenated solvents. Complexes **2**, **3**, and **5–7** are stable in chloroform-*d*₁ solutions at room temperature for several days according to ¹H NMR spectroscopy. However, the lanthanum derivative **4** in chloroform-*d*₁ immediately undergoes partial dissociation (ca. 15%) to give complex **1** and presumably [LaCl₃]. This mixture remains unaltered for long periods of time at room temperature.

Compounds **2–7** may also be prepared by the direct reaction of **1** with 1 equiv of the anhydrous metal chlorides [MCl₃] in toluene or toluene-THF mixtures, but the complexes appear invariably accompanied by significant amounts of the [MCl₃] reagent according to microanalytical data. In contrast, the analogous reaction of **1** with anhydrous yttrium, samarium, or erbium trifluoromethanesulfonate derivatives [M(O₃SCF₃)₃] in toluene afforded the precipitation of the corresponding pure triflate complexes [(CF₃SO₂O)₃M{($\mu_3\text{-NH}$)₃Ti₃($\eta^5\text{-C}_5\text{Me}_5$)₃($\mu_3\text{-N}$)}] (M = Y (**8**), Sm (**9**), Er (**10**)) (Scheme 1). Compounds **8–10** were isolated as orange solids in good yields (72–81%) which are only soluble in halogenated solvents. The preparative reactions for compounds **8** and **10** were carried out in

Scheme 1. Reactions of **1** with [MCl₃(thf)_{*n*}] or [M(OTf)₃]



toluene or toluene-THF solutions. However, the samarium complex **9** was prepared in toluene since the presence of THF in the reaction afforded a yellow solid which is not soluble in common organic solvents. Similarly, the treatment of **1** with the lanthanum triflate derivative [La(O₃SCF₃)₃] in toluene-THF mixtures gave a yellow precipitate with negligible solubility. Although the C, H, N, S microanalytical data were not fully consistent for the solids isolated from several preparative reactions, the analytical results were always close to products containing metalloligand:metal triflate ratios of 1:2. Most likely the compounds contain triflate groups bridging the large samarium or lanthanum atoms as those reported in the literature for lanthanide complexes.^{25,34} Interestingly, the addition of **1** (1 equiv) to a suspension of the samarium precipitate in chloroform-*d*₁ and subsequent heating at 70 °C overnight afforded an orange solution of complex **9** according to NMR spectroscopy.

Complexes **2–10** were characterized by spectroscopic and analytical methods, as well as by X-ray crystal structure determinations for the scandium (**2**), erbium (**6**), and lutetium (**7**) chloride derivatives. IR spectra (KBr) of the chloride derivatives **2–7** show one ν_{NH} vibration, between 3331 and 3310 cm⁻¹, whereas the IR spectra of the triflate complexes **8–10** reveal two ν_{NH} vibrations, between 3329 and 3289 cm⁻¹, in a similar range to the value determined for **1** (3352 cm⁻¹).⁴ In addition, the infrared spectra of **8–10** show several strong absorptions between 1339 and 1010 cm⁻¹ for the trifluoromethanesulfonate groups.³⁵ The bands around 1338 cm⁻¹, which are assignable to the $\nu_{\text{as}}(\text{SO}_3)$ vibrations, are shifted to higher wavenumbers than that near 1270 cm⁻¹ characteristic of the ionic CF₃SO₃⁻,^{35b} and are indicative of coordinated triflate ligands.^{35a} The ¹H and ¹³C{¹H} NMR spectra in chloroform-*d*₁ at room temperature of the diamagnetic complexes **2–4**, **7**, and **8** reveal resonance signals for equivalent NH and $\eta^5\text{-C}_5\text{Me}_5$ groups, and agree with a C_{3v} symmetric structure in solution. The NH resonance signal in the ¹H NMR spectra (δ = 13.37–12.31) is shifted to higher field than that found in **1** (δ = 13.40), suggesting a tridentate coordination of the metalloligand.^{18,19} The ¹H and ¹³C{¹H} NMR spectra of the mildly paramagnetic samarium complexes **5** and **9** are very simple and analogous to those of the diamagnetic complexes. However, the NH resonance signals (δ = 13.55 and 13.87, respectively) in the ¹H NMR spectra of **5** and **9** are shifted downfield with respect to that found in **1**. All attempts to gain structural information by NMR spectroscopy of the erbium

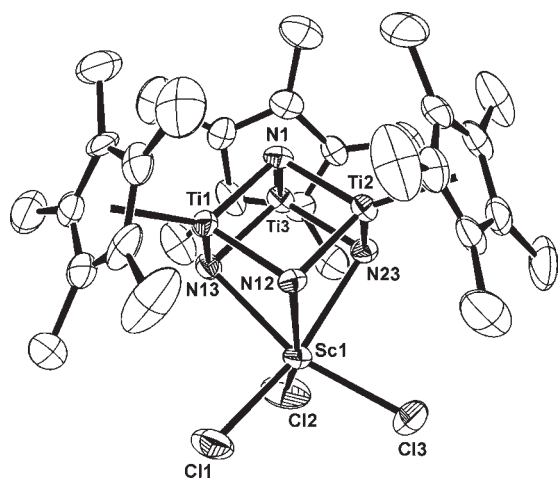


Figure 1. Perspective view with thermal ellipsoids at the 50% probability level of one of the two crystallographically independent molecules of **2**. Hydrogen atoms are omitted for clarity.

Table 2. Selected Averaged Lengths (Å) and Angles (deg) for Complexes $[\text{Cl}_3\text{M}\{\mu_3\text{-NH}\}_3\text{Ti}_3(\eta^5\text{-C}_5\text{Me}_5)_3(\mu_3\text{-N})]^{a}$

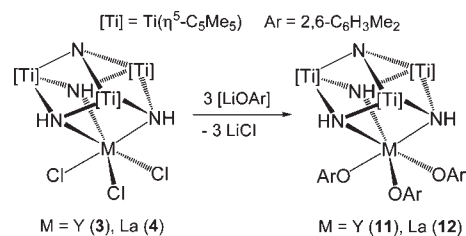
	M = Sc (2)	M = Er (6)	M = Lu (7)
M–N _{imido}	2.427(12)	2.59(3)	2.53(2)
M–Cl	2.414(8)	2.553(13)	2.516(13)
Ti–N _{imido}	1.974(14)	1.98(2)	1.978(15)
Ti–N _{nitrido}	1.930(7)	1.931(11)	1.939(8)
Ti···Ti	2.868(9)	2.869(11)	2.864(6)
M···Ti	3.219(7)	3.384(11)	3.328(8)
N _{imido} –M–N _{imido}	75.0(3)	70.5(7)	72.1(1)
Cl–M–Cl	99.1(8)	99.9(14)	99.7(11)
N _{imido} –Ti–N _{imido}	96.9(2)	98.4(7)	97.7(5)
N _{nitrido} –Ti–N _{imido}	85.4(4)	85.4(5)	86.0(5)
M–N _{imido} –Ti	93.4(4)	94.7(10)	94.3(4)
Ti–N _{imido} –Ti	93.2(1)	93.1(7)	92.8(5)
Ti–N _{nitrido} –Ti	95.9(4)	96.0(3)	95.2(5)

^a Averaged values for the two independent molecules in the asymmetric unit.

compounds **6** and **10** in solution failed because of their strong paramagnetism.

The isomorphous chloride complexes **2**, **6**,²⁰ and **7** crystallized in the space group $P2_1/c$ with two independent molecules in the asymmetric unit. There are no substantial differences between the two molecules, and the structure of one of them for the scandium chloride complex **2** is shown as example in Figure 1. Selected averaged distances and angles for the two crystallographically independent molecules of complexes **2**, **6**, and **7** are compared in Table 2. The crystal structures show $[\text{MTi}_3\text{N}_4]$ cube-type cores with the neutral ligand $[(\mu_3\text{-NH})_3\text{Ti}_3(\eta^5\text{-C}_5\text{Me}_5)_3(\mu_3\text{-N})]$ coordinating in a tripodal fashion. In all three complexes, each rare-earth center is six-coordinate, and its coordination geometry is best described as distorted trigonal antiprismatic with one tighter triangle defined by the nitrogen atoms and with a more open one defined by the chloride ligands. This is clearly seen by comparing the N–M–N [M = Sc, 75.0(3)°; Er, 70.5(7)°; Lu, 72.1(1)°] and Cl–M–Cl [M = Sc, 99.1(8)°; Er, 99.9(14)°; Lu, 99.7(11)°] averaged angles. The

Scheme 2. Synthesis of Aryloxo Derivatives



coordination environment about the rare-earth atoms in complexes **2**, **6**, and **7** is analogous to those reported for trichloride complexes containing *fac*-coordinating trinitrogen ligands such as the scandium 1,4,7-trimethyltriazacyclononane $[\text{Sc}\{\text{Me}_3[9]\text{-aneN}_3\}\text{Cl}_3]^{24a}$ and 1,3,5-trimethyltriazacyclohexane $[\text{Sc}\{\text{Me}_3[6]\text{aneN}_3\}\text{Cl}_3]^{23b}$ complexes, and the yttrium tris(pyrazolyl)silane $[\text{Y}\{\text{MeSi}(3,5\text{-Me}_2\text{pz})_3\}\text{Cl}_3]^{23b}$ and tris(pyrazolyl)methane $[\text{Y}\{\text{HC}(3,5\text{-Me}_2\text{pz})_3\}\text{Cl}_3]^{22b}$ derivatives. If the differences in ionic radii of M^{3+} in six-coordinate geometries are taken into account,³⁶ the M–Cl distances [average M = Sc, 2.414(8) Å; Er, 2.553(13) Å; Lu, 2.516(13) Å] compare well with those found in the above-mentioned examples. However, the M–N bond lengths in **2**, **6** and **7** [average M = Sc, 2.427(12) Å; Er, 2.59(3) Å; Lu, 2.53(2) Å] are clearly longer than the M–N distances in those complexes (cf. average Sc–N are 2.337(8) and 2.332(1) Å in $[\text{Sc}\{\text{Me}_3[9]\text{aneN}_3\}\text{Cl}_3]$ and $[\text{Sc}\{\text{Me}_3[6]\text{aneN}_3\}\text{-Cl}_3]$, respectively), suggesting a weaker coordination of the titanium tripodal ligand. This might be caused by the steric repulsion between the bulky pentamethylcyclopentadienyl ligands and the chloride groups placed in an eclipsed position. Accordingly, the distortions in bond distances and angles within the tridentate ligand are small when compared to those of **1**.⁶

Despite several data collections, crystals of the triflate compounds **8**–**10** presented severe disorder precluding an accurate determination of their molecular structure by crystallographic methods. However, the treatment of yttrium (**3**) or lanthanum (**4**) chloride complexes with 3 equiv of lithium 2,6-dimethylphenoxido $[\text{LiOAr}]$ in toluene gave the analogous aryloxo derivatives $[(\text{ArO})_3\text{M}\{(\mu_3\text{-NH})_3\text{Ti}_3(\eta^5\text{-C}_5\text{Me}_5)_3(\mu_3\text{-N})\}]$ (M = Y (**11**), La (**12**)) (Scheme 2), and the solid-state structure of **11** was unambiguously determined. Compounds **11** and **12** were isolated in good yields (95 and 82%, respectively) as yellow solids which exhibit an enhanced solubility in benzene and toluene when compared with the triflate derivatives **8**–**10**.

Complexes **11** and **12** were characterized by spectroscopic and analytical methods, as well as by an X-ray crystal structure determination for the yttrium derivative $\text{11} \cdot 0.5\text{C}_6\text{H}_{14}$. Spectroscopic data of **11** and **12** are similar to those of complexes **2**–**10**. ¹H and ¹³C{¹H} NMR spectra in chloroform-*d*₁ at room temperature show resonances for equivalent NH and $\eta^5\text{-C}_5\text{-Me}_5$ groups, and are consistent with a C_{3v} symmetry in solution. In addition, the spectra reveal resonance signals for three equivalent 2,6-dimethylphenoxido ligands coordinated to the yttrium or lanthanum centers.

The X-ray crystal structure of **11** is presented in Figure 2, and selected distances and angles are given in Table 3. The molecular structure shows a distorted $[\text{YTi}_3\text{N}_4]$ cube-type core similar to those of the chloride complexes **2**, **6**, and **7**. Yttrium is bonded to three oxygen atoms of the aryloxo ligands and three imido groups of the $[\text{Ti}_3(\mu\text{-NH})_3(\mu_3\text{-N})]$ fragment. The Y–O

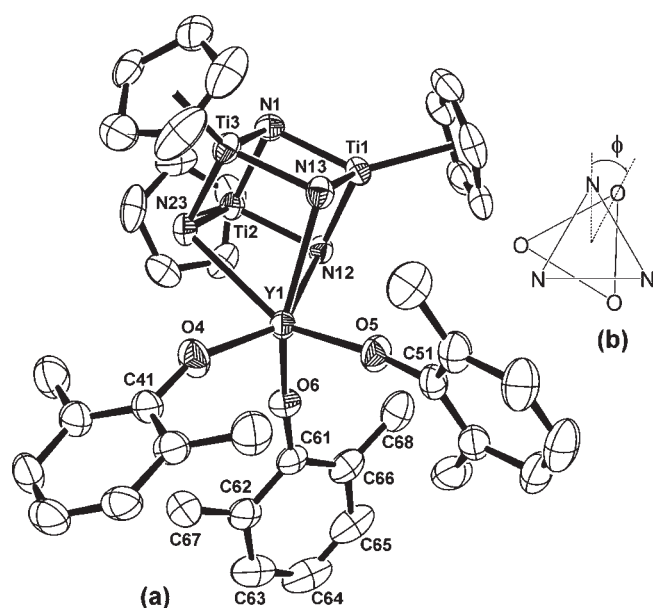


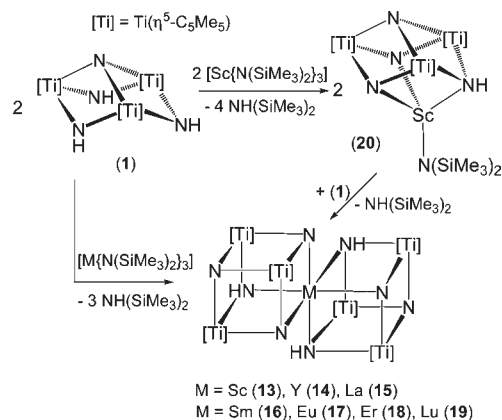
Figure 2. (a) Perspective view of **11** with thermal ellipsoids at the 50% probability level. Methyl groups of the pentamethylcyclopentadienyl ligands and hydrogen atoms are omitted for clarity. (b) Schematic representation of the six-coordinate geometry about the yttrium center in **11**.

Table 3. Selected Lengths (Å) and Angles (deg) for **11**

Y(1)–N(12)	2.629(2)	Y(1)–O(4)	2.109(2)
Y(1)–N(13)	2.618(2)	Y(1)–O(5)	2.109(2)
Y(1)–N(23)	2.662(2)	Y(1)–O(6)	2.111(2)
Ti–N _{imido} (av)	1.943(10)	Ti–N(1) (av)	1.912(1)
Ti···Ti (av)	2.823(4)	Ti···Y(1) (av)	3.427(15)
N(12)–Y(1)–N(13)	68.1(1)	O(4)–Y(1)–O(5)	102.4(1)
N(13)–Y(1)–N(23)	67.8(1)	O(4)–Y(1)–O(6)	102.9(1)
N(12)–Y(1)–N(23)	67.9(1)	O(5)–Y(1)–O(6)	101.2(1)
Y(1)–O(4)–C(41)	157.3(2)	Y(1)–O(5)–C(51)	171.9(2)
Y(1)–O(6)–C(61)	165.4(2)	N _{imido} –Ti–N _{imido} (av)	98.5(3)
N _{imido} –Ti–N(1) (av)	85.8(3)	Ti–N _{imido} –Ti (av)	93.2(1)
Ti–N _{imido} –Y(1) (av)	95.7(6)	Ti–N(1)–Ti (av)	95.1(2)

distances (average 2.110(1) Å) are in the range typical of terminal yttrium 2,6-dimethylphenoxidos,³⁷ and compare well with the M–O bond lengths determined in the crystal structures of complexes [M{HC(3,5-Me₂pz)₃}(OAr)₃] [average M = Sc,^{23b} 1.962(2) Å; M = Nd,^{22b} 2.207(5) Å; M = Sm,^{22b} 2.180(3) Å] after correction of the difference in ionic radii.³⁶ However, the Y–N bond lengths in **11** (2.618(2)–2.662(2) Å) are longer than expected from the M–N distances found in those complexes [M{HC(3,5-Me₂pz)₃}(OAr)₃] (M = Sc, 2.354(2) Å; M = Nd, 2.599(5) Å; M = Sm, 2.565(5) Å). This might be caused by the steric repulsion between the bulky pentamethylcyclopentadienyl ligands and the 2,6-dimethylphenoxido groups. The minimization of this repulsion might also explain the coordination geometry about the yttrium atom in **11**, which is best described as intermediate between trigonal prismatic and antiprismatic. This is clearly seen when one looks perpendicularly down onto the triangle defined by the nitrogen atoms and that defined by the oxygen atoms, and finds that the average twist

Scheme 3. Reactions of **1** with [M{N(SiMe₃)₂}]₃



angle ϕ , measured in the plane of projection, between those triangular faces is 32(1)° (Figure 2).³⁸ For comparison, the analogous twist angle ϕ in the chloride complexes **2**, **6**, and **7** spans 34(3)–54(2)°, and therefore the coordination geometry about the rare-earth center in those complexes is somewhat closer to trigonal antiprismatic ($\phi = 60^\circ$).

Reactions with Rare-Earth Metal Amido Derivatives. The synthetic chemistry is outlined in Scheme 3. Treatment of **1** with group 3 or lanthanide bis(trimethylsilyl)amido derivatives [M{N(SiMe₃)₂}]₃ in toluene at 85–180 °C afforded the corner-shared double-cube nitrido complexes [M(μ_3 -N)(μ_3 -NH)₃–{Ti₃(η^5 -C₅Me₅)₃(μ_3 -N)}₂] (M = Sc (**13**), Y (**14**), La (**15**), Sm (**16**), Eu (**17**), Er (**18**), Lu (**19**)) in good yields (51–86%). Compound **14** was also prepared by the reaction of **1** with 1 equiv of the yttrium alkyl derivative [Y(CH₂SiMe₃)₃(thf)₃]. Whereas the reaction of **1** with the triamido reagent [Y{N(SiMe₃)₂}]₃ is very slow at room temperature, complex **1** reacted almost immediately with the yttrium trialkyl derivative. The reactions in benzene-*d*₆ were monitored by NMR spectroscopy but no soluble intermediates were detected, and the final spectra revealed only resonances assigned to free bis(trimethylsilyl)amine or tetramethylsilane.

Complexes **13**–**19** are not soluble in common organic solvents, and their lack of volatility precludes their characterization by mass spectrometry (EI, 70 eV). Therefore, the compounds were characterized by IR spectroscopy and C, H, N microanalysis, as well as by X-ray crystal structure determinations for **14**, **15**, and **19**. Crystals of **13**–**19** contain two (**13**, **14**, **18**, **19**), one (**16**), or zero (**15**, **17**) toluene molecules per double-cube unit according to crystallographic or analytical data. However, once the crystals are separated from the solution, the toluene solvent molecules are gradually lost within hours at room temperature. The molecular structures of **15** and **19** are presented in Figures 3 and 4, while selected distances and angles of complexes **14**, **15**, and **19** are compared in Table 4. The structures confirm the expected corner-shared double-cube [MTi₆N₈] cores similar to those found in our previous studies with transition^{18b} or main-group³⁹ metals. The six-coordinate geometry about the yttrium, lanthanum, or lutetium centers is best described as trigonal antiprismatic, whereby the two tridentate organometallic ligands adopt a mutually staggered disposition. The coordination environment about the rare-earth centers resembles those determined for hydrotris(pyrazolyl)borate lanthanide(II) complexes [Ln{HB(3,5-Me₂pz)₃}]₂⁴⁰ and the

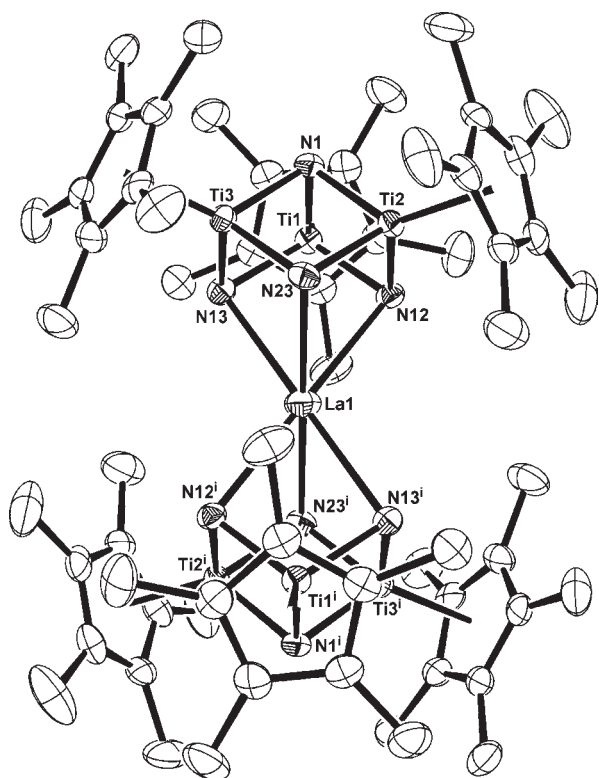


Figure 3. Perspective view of **15** with thermal ellipsoids at the 50% probability level. Hydrogen atoms are omitted for clarity. Symmetry code: (i) $1/2 - x, 1/2 - y, -z$.

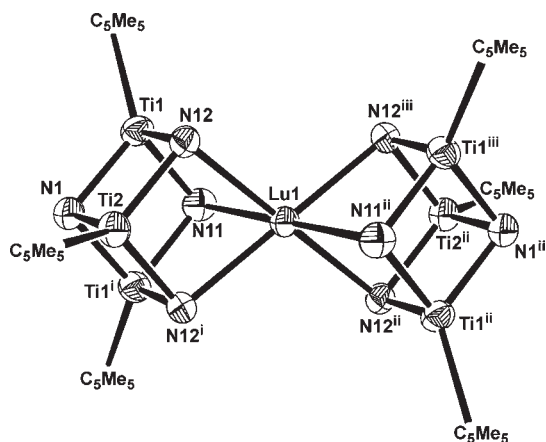


Figure 4. Simplified view of **19** with thermal ellipsoids at the 50% probability level. Pentamethylcyclopentadienyl rings and hydrogen atoms are omitted for clarity. Symmetry code: (i) $x, y, -z$; (ii) $2 - x, -y, -z$; (iii) $2 - x, -y, z$.

lanthanide(III) compounds $[\text{Ln}\{\text{HB}(3,5\text{-Me}_2\text{pz})_3\}_2]\text{X}$.⁴¹ Within the tridentate ligands, the titanium–nitrogen bond lengths and the titanium–nitrogen–titanium angles in complexes **14**, **15**, and **19** are very similar and compare well with those determined for **1**.⁶

Complexes **14**–**19** were invariably obtained by treatment of **1** with 0.5 or 1 equiv of the triamido reagents $[\text{M}\{\text{N}(\text{SiMe}_3)_2\}_3]$ at different temperatures, but the reaction of **1** with 1 equiv of $[\text{Sc}\{\text{N}(\text{SiMe}_3)_2\}_3]$ in toluene at 100 °C afforded the monoamido

Table 4. Selected Averaged Lengths (Å) and Angles (deg) for Complexes **14**, **15**, and **19**

	M = Y (14)	M = La (15)	M = Lu (19)
M–N	2.439(4)	2.601(11)	2.381(15)
Ti–N	1.952(9)	1.947(9)	1.960(10)
M···Ti	3.251(5)	3.417(9)	3.200(4)
Ti···Ti	2.821(2)	2.806(8)	2.825(1)
Ti–N–Ti	92.5(4)	92.2(3)	92.4(7)
N(1)–Ti–N	87.4(2)	87.7(2)	87.6(2)
N–Ti–N	96.0(2)	97.2(1)	95.2(6)
N–M–N ^a	73.1(1)	68.4(1)	75.1(1)
	106.9(1)	111.6(1)	104.9(1)
Ti–N–M	94.8(2)	96.3(5)	94.3(4)

^a Narrower values correspond to intracube and wider values to intercube N–M–N angles.

scandium derivative $[\{(\text{Me}_3\text{Si})_2\text{N}\}\text{Sc}\{(\mu_3\text{-N})_2(\mu_3\text{-NH})\text{Ti}_3(\eta^5\text{-C}_5\text{Me}_5)_3(\mu_3\text{-N})\}]$ (**20**) (Scheme 3). Complex **20** is stable at high temperatures in benzene-*d*₆ solution according to NMR spectroscopy. However, upon addition of 1 equiv of **1** to this solution and subsequent heating at 180 °C the spectra showed resonances assigned to $\text{NH}(\text{SiMe}_3)_2$ along with a red precipitate characterized as compound **13**.

Complex **20** was obtained in 88% yield as a red solid, which is very soluble in toluene and hexane, and was characterized by spectroscopic and analytical methods. The ¹H NMR spectrum in benzene-*d*₆ at room temperature reveals two resonances for $\eta^5\text{-C}_5\text{Me}_5$ ligands in a 1:2 ratio, a singlet for one $\text{N}(\text{SiMe}_3)_2$ group, and a broad signal for the NH imido ligand. These NMR data are consistent with a *C*_s-symmetric structure in solution as those reported for the monoamido^{39b} or monoalkyl^{19c} aluminum(III) derivatives $[\text{RAl}\{(\mu_3\text{-N})_2(\mu_3\text{-NH})\text{Ti}_3(\eta^5\text{-C}_5\text{Me}_5)_3(\mu_3\text{-N})\}]$ (R = N(SiMe₃)₂, Me, CH₂SiMe₃).

Thermal Decomposition of Heterometallic Double-Cube Nitrido Complexes. The thermal stabilities in the solid-state of complexes $[\text{M}(\mu_3\text{-N})_3(\mu_3\text{-NH})_3\{\text{Ti}_3(\eta^5\text{-C}_5\text{Me}_5)_3(\mu_3\text{-N})\}_2]$ (M = Y (**14**), La (**15**), Er (**18**)) were examined as representative examples of the large number of corner-shared double-cube nitrido derivatives reported by our laboratory.^{18b,39} This type of compounds was chosen because they are not volatile as determined by mass spectrometry (EI, 70 eV) and sublimation experiments under vacuum conditions. Therefore, any mass loss in the decomposition would be due to thermal degradation of the complexes.

Initially, the decomposition behavior of crystalline samples of compounds **14**·C₇H₈, **15**, and **18**·C₇H₈ under an argon flow was investigated by simultaneous thermogravimetric analysis (TGA) and differential thermal analysis (DTA) experiments. The volatile components generated in the degradation of the complexes were analyzed by coupled mass spectrometry (MS). The TGA and DTA curves for the yttrium derivative **14**·C₇H₈ are shown in Figure 5 (Figures S3 and S4 in the Supporting Information show the TGA/DTA curves for **15** and **18**·C₇H₈). The TGA curves for **14**·C₇H₈ and **18**·C₇H₈ display a weight loss of ≈7 and 6%, respectively, between 120 and 190 °C (endothermic peaks at 159 and 140 °C in the DTA curves, respectively), which cannot be observed during the decomposition of the lanthanum complex **15**. These mass losses at the very beginning of the decomposition are due to release of toluene solvent molecules of crystallization, which are absent in **15**. The

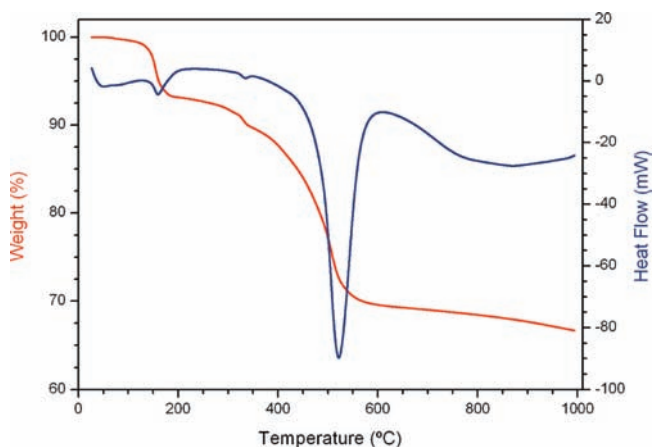


Figure 5. TGA (red) and DTA (blue) curves for the degradation of $14 \cdot C_7H_8$ under Ar flow at a heating rate of $10 \text{ }^\circ\text{C}/\text{min}$.

elimination of toluene was unambiguously established by MS (m/z 92) while the theoretical mass loss for one toluene molecule from compounds $14 \cdot C_7H_8$ and $18 \cdot C_7H_8$ is 6.6 and 6.3%, respectively. The main mass loss (20–23%) for the three complexes starts at about $200 \text{ }^\circ\text{C}$ and is finished around $600 \text{ }^\circ\text{C}$ (endothermic peaks at $514\text{--}522 \text{ }^\circ\text{C}$ in the DTA curves). Analysis of the volatile components generated in this step by MS revealed fragments derived of the C_5Me_5 groups (m/z 135 $[C_5Me_5]^+$, 119 $[C_5Me_3CH_2]^+$, 16 $[CH_4]^+$, 15 $[CH_3]^+$). Between 600 and $1000 \text{ }^\circ\text{C}$ the TGA curves show additional mass losses of about 3% to give black residues containing 67, 73, or 70% of the initial mass of compounds $14 \cdot C_7H_8$, **15**, and $18 \cdot C_7H_8$, respectively. These results suggest that a considerable amount of carbon arising from the C_5Me_5 groups should be present in the residues, which were found amorphous by powder X-ray diffraction. Elemental analysis of the black solid obtained in the TGA of **14** demonstrated those high levels of carbon (41.9%) along with lower levels of hydrogen and nitrogen (0.7 and 5.1%, respectively).

The pyrolysis of the yttrium compound $14 \cdot C_7H_8$ under different atmospheres was investigated (Ar, H_2/N_2 , NH_3) in more detail. Heating under an argon flow (100 sccm) from 20 to $1100 \text{ }^\circ\text{C}$ gave rise to a black powder (63% of the initial mass), which was found to contain high levels of carbon (48.8%) by elemental analysis (Table 5). Compositional analysis by energy dispersive analysis of X-rays (EDX) shows the presence of titanium and yttrium in the solid (see the Supporting Information). The ceramic yield and large amounts of carbon derived of the C_5Me_5 groups in the resultant product are consistent with those obtained in the TGA experiment under argon for this compound.

The pyrolysis of $14 \cdot C_7H_8$ from room temperature to $1100 \text{ }^\circ\text{C}$ was also carried out under a flow (100 sccm) of H_2/N_2 (6–15% H_2) to give a black residue with 58% of the initial mass. Elemental analysis of this solid reveals about 42.7% of carbon and 9.4% of nitrogen, whereas the EDX measurement shows the presence of titanium and yttrium. The volatile byproduct of the decomposition were trapped at $-196 \text{ }^\circ\text{C}$ (liquid nitrogen bath), and after closing the flow of gas, benzene- d_6 was injected into the cooling trap. The resulting C_6D_6 solution was analyzed by 1H NMR spectroscopy and GC-MS measurements, and C_5Me_5H was unambiguously identified in both techniques. It appears that

Table 5. Ceramic Yields and Characteristics of the Pyrolyzed Products of $14 \cdot C_7H_8$

experiment	color	ceramic yield (%)	elemental analysis (%) ^a			
			C	H	N	O
Ar flow ^b	black	63	48.8	0.3	5.1	3.9
H_2/N_2 flow ^b	black	58	42.7	0.5	9.4	4.0
NH_3 flow ^b	iridescent garnet	55	22.9	0.4	13.2	1.5
NH_3 flow ^c	iridescent garnet	32	0.2	0.3	18.0	0.2

^a Averaged values from at least two independent samples. ^b 100 sccm. ^c 1350 sccm.

the potentially reactive H_2/N_2 atmosphere somewhat facilitates the elimination of the organic groups, but the ceramic yield and carbon content of the residue are still very high.

Finally, pyrolyses of $14 \cdot C_7H_8$ from 20 to $1100 \text{ }^\circ\text{C}$ were performed under different flows of anhydrous ammonia. While the decomposition of **14** under a flow of NH_3 of 100 sccm gave an iridescent garnet solid with 55% of the initial mass, a higher flow of NH_3 (1350 sccm) afforded a residue mass of 32%, which is closer to the calculated mass for complete degradation to “ YTi_6N_8 ” (35%) or “ YTi_6N_7 ” (34%). Accordingly, the residue obtained in the former experiment still contains high levels of carbon (22.9% by elemental analysis) and low levels of nitrogen (13.2%), while the solid isolated under a large flow of ammonia has only a very small amount of carbon (0.2%) along with a nitrogen content (18.0%) closer to the expected values for YTi_6N_8 or YTi_6N_7 compositions (23.0 and 20.7%, respectively).

The garnet solid obtained under a large flow of NH_3 was studied in more detail. Elemental analyses reveal very low hydrogen and oxygen levels (0.3 and 0.2%, respectively), whereas compositional analysis by EDX confirms the presence of titanium and yttrium in the solid. PXRD analysis showed that the residue was essentially amorphous, and only weak peaks could be assigned to TiN and Y_2O_3 . Rare-earth nitrides exhibit a high reactivity toward air to give the metal oxides,⁴² and minor oxidation/hydrolysis of the sample might explain the Y_2O_3 detection in the XRD experiment. Indeed, the elemental analysis of a sample exposed to air for 20 h at room temperature gave an increased oxygen content (1.3%) without any significant variation on the C, H, and N levels (0.4, 0.0 and 18.3%, respectively).

The ceramic yield and the negligible carbon content in this residue agree with an efficient removal of the C_5Me_5 groups in the precursor, probably via acid–base reactions with NH_3 . We are currently investigating the pyrolysis under NH_3 at different conditions (e.g., lower temperatures and slower heating rates) of compound **14** and other cube-type heterometallic nitrido complexes to optimize the preparation and characterization of metal nitride materials.

CONCLUSION

We have presented the systematic syntheses of a series of well-characterized titanium-group 3/lanthanide molecular nitrides by reaction of the imido-nitrido titanium complex **1** with several derivatives of the rare-earth metals. Complex **1** is capable of acting as a neutral facially coordinating ligand to metal halide, triflate or aryloxy derivatives to give single-cube complexes $[X_3M\{\mu_3-NH\}_3Ti_3(\eta^5-C_5Me_5)_3(\mu_3-N)]$. Analogous treatment with metal triamido reagents produces the deprotonation of **1** to yield corner-shared double-cube nitrido derivatives

$[M(\mu_3\text{-N})_3(\mu_3\text{-NH})_3\{\text{Ti}_3(\eta^5\text{-C}_5\text{Me}_5)_3(\mu_3\text{-N})\}_2]$ and the corresponding amine molecules. Thermal decomposition experiments (TGA/DTA and pyrolysis) carried out on selected double-cube compounds under argon atmosphere give black residues containing large amounts of carbon because of inefficient removal of the pentamethylcyclopentadienyl ligands. However, the pyrolysis of the yttrium double-cube derivative **14** at 1100 °C under NH_3 leads to the formation of a metal nitride material with a negligible carbon level.

■ ASSOCIATED CONTENT

S Supporting Information. Perspective views of the molecular structure of complexes **7** and **14**, TGA/TDA curves for complexes **15** and **18**, TGA-MS spectra, EDX spectra of solids obtained in the thermal decomposition of **14**, and PXRD spectrum of the solid obtained in the pyrolysis of **14** under a large flow of NH_3 (PDF). X-ray crystallographic files in CIF format for complexes **2**, **7**, **11**, **14**, **15**, and **19**. This material is available free of charge via the Internet at <http://pubs.acs.org>.

■ AUTHOR INFORMATION

Corresponding Author

*Fax: (+34) 91-8854683. E-mail: carlos.yelamos@uah.es.

■ ACKNOWLEDGMENT

We thank Dr. Rosa Rojas of the ICMM for assistance with the TGA/DTA experiments. We are also grateful to the Spanish MEC (CTQ2008-00061/BQU), Comunidad de Madrid and the Universidad de Alcalá (CCG10-UAH/PPQ-5935), and the Factoría de Cristalización (CONSOLIDER-INGENIO 2010 CSD2006-00015) for financial support of this research. J.C. thanks the MEC for a doctoral fellowship.

■ REFERENCES

- (1) (a) Dehnicke, K.; Strähle, J. *Angew. Chem., Int. Ed. Engl.* **1981**, *20*, 413–426. (b) Dehnicke, K.; Strähle, J. *Angew. Chem., Int. Ed. Engl.* **1992**, *31*, 955–978. (c) Dehnicke, K.; Weller, F.; Strähle, J. *Chem. Soc. Rev.* **2001**, *30*, 125–135.
- (2) (a) Nugent, W. A.; Mayer, J. M. *Metal-Ligand Multiple Bonds*; Wiley: New York, 1988. (b) Eikey, R. A.; Abu-Omar, M. M. *Coord. Chem. Rev.* **2003**, *243*, 83–124.
- (3) For selected examples of dinuclear early transition-metal nitrido derivatives, see: (a) Haddad, T. S.; Aistars, A.; Ziller, J. W.; Doherty, N. M. *Organometallics* **1993**, *12*, 2420–2422. (b) Berno, P.; Gambarotta, S. *Angew. Chem., Int. Ed. Engl.* **1995**, *34*, 822–824. (c) Song, J.-I.; Gambarotta, S. *Chem.—Eur. J.* **1996**, *2*, 1258–1263. (d) Tayebani, M.; Feghali, K.; Gambarotta, S.; Bensimon, C. *Organometallics* **1997**, *16*, 5084–5088. (e) Clentsmith, G. K. B.; Bates, V. M. E.; Hitchcock, P. B.; Cloke, F. G. N. *J. Am. Chem. Soc.* **1999**, *121*, 10444–10445. (f) Gauch, E.; Hoppe, H.; Strähle, J. *J. Organomet. Chem.* **2000**, *593*, 175–179. (g) Carmalt, C. J.; Mileham, J. D.; White, A. J. P.; Williams, D. J. *New J. Chem.* **2000**, *24*, 929–930. (h) Hirotsu, M.; Fontaine, P. P.; Epshteyn, A.; Zavalij, P.; Sita, L. R. *J. Am. Chem. Soc.* **2007**, *129*, 9284–9285. (i) Akagi, F.; Matsuo, T.; Kawaguchi, H. *Angew. Chem., Int. Ed.* **2007**, *46*, 8778–8781. (j) Nikiforov, G. B.; Vidyaratne, I.; Gambarotta, S.; Korobkov, I. *Angew. Chem., Int. Ed.* **2009**, *48*, 7415–7419.
- (4) Abarca, A.; Gómez-Sal, P.; Martín, A.; Mena, M.; Poblet, J.-M.; Yélamos, C. *Inorg. Chem.* **2000**, *39*, 642–651.
- (5) (a) Plenio, H.; Roesky, H. W.; Noltemeyer, M. *Angew. Chem., Int. Ed. Engl.* **1988**, *27*, 1330–1331. (b) Banaszak Holl, M. M.; Kersting, M.;

- Pendley, B. D.; Wolczanski, P. T. *Inorg. Chem.* **1990**, *29*, 1518–1526. (c) Duan, Z.; Verkade, J. G. *Inorg. Chem.* **1996**, *35*, 5325–5327. (d) Mindiola, D. J.; Meyer, K.; Cherry, J.-P. F.; Baker, T. A.; Cummins, C. C. *Organometallics* **2000**, *19*, 1622–1624.
- (6) Roesky, H. W.; Bai, Y.; Noltemeyer, M. *Angew. Chem., Int. Ed. Engl.* **1989**, *28*, 754–755.
 - (7) (a) Gómez-Sal, P.; Martín, A.; Mena, M.; Yélamos, C. *J. Chem. Soc., Chem. Commun.* **1995**, 2185–2186. (b) Abernethy, C. D.; Bottomley, F.; Decken, A.; Cameron, T. S. *Organometallics* **1996**, *15*, 1758–1759. (c) Fickes, M.; Odum, A. L.; Cummins, C. C. *Chem. Commun.* **1997**, 1993–1994.
 - (8) (a) Banaszak Holl, M. M.; Wolczanski, P. T.; Van Duyne, G. D. *J. Am. Chem. Soc.* **1990**, *112*, 7989–7994. (b) Banaszak Holl, M. M.; Wolczanski, P. T. *J. Am. Chem. Soc.* **1992**, *114*, 3854–3858. (c) Bai, G.; Müller, P.; Roesky, H. W.; Usón, I. *Organometallics* **2000**, *19*, 4675–4677. (d) Bai, G.; Roesky, H. W.; Müller, P. *Bull. Pol. Acad. Sci.-Chem.* **2002**, *50*, 1–10.
 - (9) Bai, G.; Roesky, H. W.; Noltemeyer, M.; Hao, H.; Schmidt, H.-G. *Organometallics* **2000**, *19*, 2823–2825.
 - (10) (a) Lee, S. C.; Holm, R. H. *Proc. Natl. Acad. Sci. U.S.A.* **2003**, *100*, 3595–3600. (b) Lee, S. C.; Holm, R. H. *Chem. Rev.* **2004**, *104*, 1135–1157.
 - (11) (a) Kuganathan, N.; Green, J. C.; Himmel, H.-J. *New J. Chem.* **2006**, *30*, 1253–1262. (b) Himmel, H.-J.; Reiher, M. *Angew. Chem., Int. Ed.* **2006**, *45*, 6264–6288.
 - (12) (a) Gambarotta, S.; Scott, J. *Angew. Chem., Int. Ed.* **2004**, *43*, 5298–5308. (b) Spencer, L. P.; MacKay, B. A.; Patrick, B. O.; Fryzuk, M. D. *Proc. Natl. Acad. Sci. U.S.A.* **2006**, *103*, 17094–17098. (c) Fryzuk, M. D. *Acc. Chem. Res.* **2009**, *42*, 127–133.
 - (13) Oyama, S. T., Ed.; *The Chemistry of Transition Metal Carbides and Nitrides*; Blackie Academic & Professional: London, 1996.
 - (14) Banaszak Holl, M. M.; Wolczanski, P. T.; Proserpio, D.; Bielecki, A.; Zax, D. B. *Chem. Mater.* **1996**, *8*, 2468–2480.
 - (15) (a) Kniep, R. *Pure Appl. Chem.* **1997**, *69*, 185–191. (b) Niewa, R.; DiSalvo, F. J. *Chem. Mater.* **1998**, *10*, 2733–2752. (c) Gregory, D. H. *J. Chem. Soc., Dalton Trans.* **1999**, 259–270. (d) Gregory, D. H. *Coord. Chem. Rev.* **2001**, *215*, 301–345.
 - (16) (a) Polarz, S.; Orlov, A.; Hoffmann, A.; Wagner, M. R.; Rauch, C.; Kirste, R.; Gehlhoff, W.; Aksu, Y.; Driess, M.; van der Berg, M. W. E.; Lehmann, M. *Chem. Mater.* **2009**, *21*, 3889–3897. (b) Heitz, S.; Epping, J.-D.; Aksu, Y.; Driess, M. *Chem. Mater.* **2010**, *22*, 4563–4571. (c) Heitz, S.; Aksu, Y.; Merschjann, C.; Driess, M. *Chem.—Eur. J.* **2011**, *17*, 3904–3910 and references therein.
 - (17) (a) Elder, S. H.; Doerr, L. H.; DiSalvo, F. J.; Parise, J. B.; Guymard, D.; Tarascon, J. M. *Chem. Mater.* **1992**, *4*, 928–937. (b) Paine, R. T.; Janik, J. F.; Fan, M. *Polyhedron* **1994**, *13*, 1225–1232. (c) Cheng, F.; Sugahara, Y.; Kuroda, K. *Appl. Organomet. Chem.* **2001**, *15*, 710–716. (d) Fan, M.; Duesler, E. N.; Janik, J. F.; Paine, R. T. *J. Inorg. Organomet. Polym. Mater.* **2007**, *17*, 423–437.
 - (18) (a) Freitag, K.; Gracia, J.; Martín, A.; Mena, M.; Poblet, J.-M.; Sarasa, J. P.; Yélamos, C. *Chem.—Eur. J.* **2001**, *7*, 3644–3651. (b) Abarca, A.; Galakhov, M.; Gracia, J.; Martín, A.; Mena, M.; Poblet, J.-M.; Sarasa, J. P.; Yélamos, C. *Chem.—Eur. J.* **2003**, *9*, 2337–2346. (c) Martín, A.; Martínez-Espada, N.; Mena, M.; Pérez-Redondo, A.; Yélamos, C. *Inorg. Chem.* **2006**, *45*, 6901–6911. (d) Martínez-Espada, N.; Mena, M.; Mosquera, M. E. G.; Pérez-Redondo, A.; Yélamos, C. *Organometallics* **2010**, *29*, 6732–6738.
 - (19) (a) García-Castro, M.; Martín, A.; Mena, M.; Yélamos, C. *Organometallics* **2004**, *23*, 1496–1500. (b) García-Castro, M.; Gracia, J.; Martín, A.; Mena, M.; Poblet, J.-M.; Sarasa, J. P.; Yélamos, C. *Chem.—Eur. J.* **2005**, *11*, 1030–1041. (c) García-Castro, M.; Martín, A.; Mena, M.; Yélamos, C. *Organometallics* **2007**, *26*, 408–416.
 - (20) Caballo, J.; García-Castro, M.; Martín, A.; Mena, M.; Pérez-Redondo, A.; Yélamos, C. *Inorg. Chem.* **2008**, *47*, 7077–7079.
 - (21) (a) Santos, I.; Marques, N. *New J. Chem.* **1995**, *19*, 551–571. (b) Marques, N.; Sella, A.; Takats, J. *Chem. Rev.* **2002**, *102*, 2137–2159.
 - (22) (a) Bigmore, H. R.; Lawrence, S. C.; Mountford, P.; Tredget, C. S. *Dalton Trans.* **2005**, 635–651. (b) Sella, A.; Brown, S. E.; Steed, J. W.; Tocher, D. A. *Inorg. Chem.* **2007**, *46*, 1856–1864.

(23) (a) Lawrence, S. C.; Ward, B. D.; Dubberley, S. R.; Kozak, C. M.; Mountford, P. *Chem. Commun.* **2003**, 2880–2881. (b) Tredget, C. S.; Lawrence, S. C.; Ward, B. D.; Howe, R. G.; Cowley, A. R.; Mountford, P. *Organometallics* **2005**, *24*, 3136–3148.

(24) (a) Hajela, S.; Schaefer, W. P.; Bercaw, J. E. *J. Organomet. Chem.* **1997**, *532*, 45–53. (b) Bambirra, S.; van Leusen, D.; Meetsma, A.; Hessen, B.; Teuben, J. H. *Chem. Commun.* **2001**, 637–638. (c) Bambirra, S.; Meetsma, A.; Hessen, B. *Acta Crystallogr.* **2006**, *E62*, m314–m316. (d) Bambirra, S.; Meetsma, A.; Hessen, B.; Bruins, A. P. *Organometallics* **2006**, *25*, 3486–3495. (e) Bambirra, S.; van Leusen, D.; Tazelaar, C. G. J.; Meetsma, A.; Hessen, B. *Organometallics* **2007**, *26*, 1014–1023.

(25) Köhn, R. D.; Pan, Z.; Kociok-Köhn, G.; Mahon, M. F. *J. Chem. Soc., Dalton Trans.* **2002**, 2344–2347.

(26) (a) Edlmann, F. T. In *Herrmann/Brauer Synthetic Methods of Organometallic and Inorganic Chemistry*; Herrmann, W. A., Ed.; Georg Thieme Verlag: New York, 1996; Vol. 6. (b) Willey, G. R.; Woodman, T. J.; Drew, M. G. B. *Polyhedron* **1997**, *16*, 3385–3393 and references therein.

(27) Wu, S. H.; Ding, Z.-B.; Li, X.-J. *Polyhedron* **1994**, *13*, 2679–2681.

(28) Lappert, M. F.; Pearce, R. *J. Chem. Soc., Chem. Commun.* **1973**, 126–126.

(29) Alyea, E. C.; Bradley, D. C.; Copperthwaite, R. G. *J. Chem. Soc., Dalton Trans.* **1972**, 1580–1584.

(30) (a) Bradley, D. C.; Ghotra, J. S.; Hart, F. A. *J. Chem. Soc., Chem. Commun.* **1972**, 349–350. (b) Bradley, D. C.; Ghotra, J. S.; Hart, F. A. *J. Chem. Soc., Dalton Trans.* **1973**, 1021–1023.

(31) Farrugia, L. J. *J. Appl. Crystallogr.* **1999**, *32*, 837–838.

(32) Sheldrick, G. M. *Acta Crystallogr.* **2008**, *A64*, 112–122.

(33) Spek, A. L. *J. Appl. Crystallogr.* **2003**, *36*, 7–13.

(34) (a) Mashima, K.; Oshiki, T.; Tani, K. *J. Org. Chem.* **1998**, *63*, 7114–7116. (b) Hitchcock, P. B.; Hulkes, A. G.; Lappert, M. F.; Protchenko, A. V. *Inorg. Chim. Acta* **2006**, *359*, 2998–3006 and references therein.

(35) (a) Lawrance, G. A. *Chem. Rev.* **1986**, *86*, 17–33. (b) Johnston, D. H.; Shriver, D. F. *Inorg. Chem.* **1993**, *32*, 1045–1047. (c) Huang, W.; Frech, R.; Wheeler, R. A. *J. Phys. Chem.* **1994**, *98*, 100–110.

(36) Shannon, R. D. *Acta Crystallogr.* **1976**, *A32*, 751–767.

(37) (a) Evans, W. J.; Olofson, J. M.; Ziller, J. W. *Inorg. Chem.* **1989**, *28*, 4308–4309. (b) Evans, W. J.; Ansari, M. A.; Ziller, J. W.; Khan, S. I. *J. Organomet. Chem.* **1998**, *553*, 141–148.

(38) (a) Cotton, F. A.; Wilkinson, G.; Murillo, C.; Bochmann, M. *Advanced Inorganic Chemistry*, 6th ed.; John Wiley & Sons: New York, 1999; pp 6–7. (b) Fleischer, E. B.; Gebala, A. E.; Swift, D. R.; Tasker, P. A. *Inorg. Chem.* **1972**, *11*, 2775–2784. (c) El-Kurdi, S.; Seppelt, K. *Chem.—Eur. J.* **2011**, *17*, 3956–3962.

(39) (a) Martín, A.; Mena, M.; Pérez-Redondo, A.; Yélamos, C. *Inorg. Chem.* **2004**, *43*, 2491–2498. (b) García-Castro, M.; Martín, A.; Mena, M.; Yélamos, C. *Chem.—Eur. J.* **2009**, *15*, 7180–7191.

(40) (a) Takats, J.; Zhang, X. W.; Day, V. W.; Eberspacher, T. A. *Organometallics* **1993**, *12*, 4286–4288. (b) Maunder, G. H.; Sella, A.; Tocher, D. A. *J. Chem. Soc., Chem. Commun.* **1994**, 885–886.

(41) (a) Liu, S.-Y.; Maunder, G. H.; Sella, A.; Stevenson, M.; Tocher, D. A. *Inorg. Chem.* **1996**, *35*, 76–81. (b) Hillier, A. C.; Zhang, X. W.; Maunder, G. H.; Liu, S. Y.; Eberspacher, T. A.; Metz, M. V.; McDonald, R.; Domingos, A.; Marques, N.; Day, V. W.; Sella, A.; Takats, J. *Inorg. Chem.* **2001**, *40*, 5106–5116. (c) Han, F.; Zhang, J.; Yi, W.; Zhang, Z.; Yu, J.; Weng, L.; Zhou, X. *Inorg. Chem.* **2010**, *49*, 2793–2798.

(42) (a) LaDuca, R. L.; Wolczanski, P. T. *Inorg. Chem.* **1992**, *31*, 1311–1313. (b) Fitzmaurice, J. C.; Hector, A.; Rowley, A. T.; Parkin, I. P. *Polyhedron* **1994**, *13*, 235–240. (c) Thiede, T. B.; Krasnopolski, M.; Milanov, A. P.; de los Arcos, T.; Ney, A.; Becker, H.-W.; Rogalla, D.; Winter, J.; Devi, A.; Fischer, R. A. *Chem. Mater.* **2011**, *23*, 1430–1440.